Physica I, pp. 689-704 (1934), translated by Anthony Yen *

DIFFRACTION THEORY OF THE KNIFE-EDGE TEST AND ITS IMPROVED FORM, THE PHASE-CONTRAST METHOD

F. ZERNIKE

Physical Laboratory of University of Groningen

Abstract

On the basis of Abbe's diffraction theory of optical imaging, the appearance of a concave mirror with arbitrarily shaped small deviations is evaluated with Foucault's knife-edge test and the new phase-contrast procedure. The orthogonal "circle polynomials" are found and applied to the diffraction phenomena of circular mirrors.

The well-known knife-edge test for the testing of concave mirrors, or more generally of optical systems, was introduced by Foucault in 1859 [1].

A spherical concave mirror is set up in such a way that it forms an image of a point source displaced somewhat laterally from its center of curvature. One then views the mirror surface by placing his eye closely behind this image. Small figure errors of the mirror remain invisible, the surface appears uniformly bright. However the errors become visible if one masks the image of the light source partially by a laterally inserted knife-edge.

Foucault explained the principle of this test by means of geometrical optics. A diffraction theoretical treatment is obviously preferred, and in fact is the only possible one if one deals with very small deviations of the mirror surface from the ideal form, or the determination of the limit of sensitivity of the method.

Until now it has apparently not been recognized that such a diffraction theory in principle already exists in Abbe's theory of microscopic imaging. Indeed the arrangements of the imaging optical systems in both cases are completely different. However, two corresponding imaging processes appear in both cases, namely the imaging of the light source and the imaging of the transilluminated object located between the light source and its image. In order to better understand the analogy, let us imagine dark stripes drawn on the mirror surface. They serve as the object on which the eye is focussed, and which is clearly visible without the knife-edge. Just as with Abbe, what matters here are the diffraction images resulting from diffraction at the object, which are located next to the direct image of the light source. According to Abbe, the outgoing light rays from these diffraction images produce the image of the object in the image plane by interference. In reality, with the mirror test, we are not concerned with dark stripes, rather with raised and lowered points on the mirror surface, i.e. with an object that causes no attenuation but only a phase change of the light, comparable to a transparent and colorless object in a microscope. Since

*The translator gratefully acknowledges contributions made by Frits Zernike, Martin Burkhardt, Bernd Geh, and Shinn-Sheng Yu to this translation.

[1] L. Foucault, Ann. Obs. Paris, **5**, 203, (1859).

such an object gives diffraction images just as well, it seems in this context initially strange that the interference of these diffraction images yields a uniformly bright surface in the image plane. Hence, the diffraction images of an absorbent and a phase-changing object must be different in some sense, though their appearance is the same. An elementary consideration [2] already shows that the difference here is that in the second case the phase of the diffraction images is shifted by 90° and no longer coincides with that of the central image. In this way an exact compensation of the intensity results in the image plane. Obviously this situation is disturbed by a partial mask with a knife-edge, or, in general, by any intervention in the diffraction images, so that errors of the mirror become visible.

It is possible to artificially compensate the phase shift between the central image and the diffraction images in a simple way. In this way the phase-changing object will be depicted as an absorbent one, i.e. the raised and lowered points of the mirror surface are reproduced as bright or dark points in the image plane. This *phase-contrast method* is evidently superior to Foucault's method [3] in several different aspects. The present work contains the more exact calculation of both methods.

2. *Setup.* The theory shall be developed for the simple case of the test of a concave mirror at its center of curvature. The setup is shown schematically in Fig. 1. A point source is situated at the center of curvature B (in practice of course displaced laterally to about B') on the optical axis AD. According to geometrical optics, the light from the mirror is recombined at B, whereas in reality the well-known small disk with rings results due to diffraction. The lens L forms an image of the mirror surface A_1A_2 in D_1D_2, which has the same curvature as the mirror (ignoring errors of the lens). Let us consider specifically the axial points A and D. A spherical wave with wavefront B_1B_2, coming from A, is inverted to C_1C_2 after passage through the lens and converges towards point D. We now choose the spherical surface B_1B_2 with A as its center as an "intermediate surface" where the diffraction image is formed (called primary image by Abbe). This choice of intermediate surface has the result that, with the ideal (here spherical) mirror, all points of the diffraction image on this surface oscillate in phase due to the symmetry of the mirror about A [4].

Now if the mirror surface has raised or lowered areas, then the phases of the light waves that combine to form the diffraction image on the spherical surface B_1B_2 change, and the resulting change in amplitude and phase of this so-called "intermediate image" shall first be calculated. This is a simple question of Fraunhofer diffraction, since B is the conjugate of the light source. With the knife-edge method, this diffraction image is partially blacked out, while it is locally altered in phase with the new "phase-contrast procedure" in order to influence the image D_1D_2 of the mirror surface favorably. The evaluation of the image in D_1D_2 from the intermediate image is in principle the same as that for the first diffraction phenomenon, it is however now to be integrated over the surface B_1B_2 and the points where the image is calculated lie on D_1D_2, conjugated to A_1A_2. Furthermore, the optical path length $A_1B_1D_1$ is independent of the position of point B,

[2] F. Zernike, Monthly Not. R. Astron. Soc. **94**, 377 (1934).

[3] C. R. Burch, Monthly Not. R. Astron. Soc. **94**, 384 (1934).

[4] The artifice of spherical intermediate surface originates from O. Lummer and F. Reiche, Die Lehre von der Bildentstehung im Mikroskop, Braunschweig 1910, §§13 and 25.

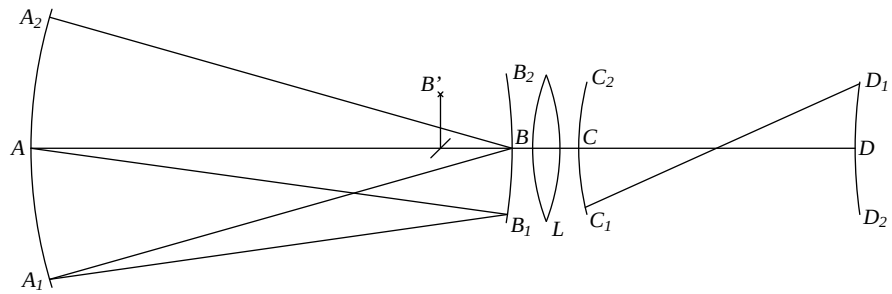

Figure 1: Setup.

hence $A_1B_1 + B_1D_1 = (A_1B + BD_1)$. Since $A_1B = AB = AB_1$, therefore

$$A_1B_1 - AB_1 \quad = \quad -(B_1D_1 - BD_1) \tag{1}$$

i.e. the path length difference that is used to calculate the phase for the second diffraction is the same as that for the first diffraction with the opposite sign. Therefore the properties of the lens and the image surface (formed possibly by the observing eye) do not need to be considered any further [5].

3. *Diffraction image of mirror errors.* As a first approach let us consider a mirror surface with a rectangular boundary. We place in the mirror surface a coordinate system with x- and y-axis having its origin in the center of the mirror. The border of the mirror is given by x, $y = \pm 1$. We now consider only the x-coordinate, to simplify the formulae. The results can be easily extended to the two dimensional case.

Deviations of the mirror from the ideal shape (spherical in the case considered) cause deviations of the phase of the reflected light at these locations. Let the oscillation of light on an error-free point of the mirror be given by $A \sin \omega t$, and on an imperfect point by $A \sin(\omega t + 4\pi d/\lambda)$ if the surface there is too high by d. We decompose the oscillation into two "perpendicular" components:

$$A \sin(\omega t + 4\pi d/\lambda) \quad = \quad A \sin \omega t \cos 4\pi d/\lambda + A \cos \omega t \sin 4\pi d/\lambda$$

We assume that the deviations of the mirror from the ideal shape are small compared to the wavelength (and will maintain this assumption in what follows). This means that the phase deviation is small and that we can set approximately:

$$A \sin(\omega t + 4\pi d/\lambda) \quad \approx \quad A \sin \omega t + A \cdot 4\pi d/\lambda \cos \omega t \tag{2}$$

Therefore, there is another oscillation that is superposed on the "error-free" oscillation $A \sin \omega t$. It has a phase advancement of $\pi/2$ and an amplitude $A \cdot 4\pi d/\lambda$. This amplitude is a function of x, since the error d depends on the position x, from which the wave is reflected.

We now expand $4\pi d/\lambda$ between -1 and +1 using Legendre Polynomials:

$$\frac{4\pi}{\lambda} d(x) \quad = \quad \sum_0^\infty C_n P_n(x) \tag{3}$$

[5] Lummer and Reiche, loc. cit.

The first three terms of this series result in a constant, a linear, and a quadratic dependence of the path length, respectively. The first one is unobservable, the second and the third vanish by a suitable displacement of B in, respectively, a lateral, and an axial direction. From $C_3P_3(x)$ on the terms represent actual errors of the mirror. Since every arbitrary position dependence of d can be depicted by (3), it is sufficient to carry out all further calculations for the general member $C_nP_n(x)$, and then eventually superpose all images so obtained, i.e. make them interfere with each other.

We now compute the diffraction image caused by a mirror error $C_nP_n(x)$. We place a coordinate system x_1y_1 in the intermediate surface B_1B_2, that is parallel to the coordinate system of the mirror surface and has its origin on the optical axis of the system. As a first approach we consider here also only the x_1-coordinate, i.e. we compute the one-dimensional diffraction image of a one-dimensional mirror. The optical path length of all points x on the mirror towards $x_1 = 0$ on the intermediate surface has the same value s. The same is true for the path length from the point $x = 0$ on the mirror to all points on the curved intermediate surface. One finds in first-order approximation $s - xx_1/s$ for the optical path of a point x on the mirror surface to a point x_1 on the intermediate surface. We find the light excitation at x_1 by adding up the incoming light from all points on the mirror with the correct amplitudes and phases. The constant factor A, valid in the mirror plane, will change to B. Therefore, one finds the light excitation at x_1 due to a mirror surface error $C_nP_n(x)$ from the integral:

$$\begin{aligned} L_n(\xi) &= \int_{-1}^{+1} BC_nP_n(x)\cos\omega(t + xx_1/sc)\,dx \\ &= BC_n\cos\omega t\int_{-1}^{+1} P_n(x)\cos\xi x\,dx - BC_n\sin\omega t\int_{-1}^{+1} P_n(x)\sin\xi x\,dx \end{aligned} \tag{4}$$

where we have set $2\pi x_1/s\lambda = \xi$ for short.

Obviously for even n only the first integral is different from zero, and for odd n only the second integral. According to a well-known formula by Gegenbauer [6], one obtains here Bessel functions of half-integer indices specifically:

$$L_{2m-1}(\xi) = (-1)^m BC_{2m-1}\sin\omega t\sqrt{\frac{2\pi}{\xi}}J_{2m-\frac{1}{2}}(\xi) \tag{5}$$

$$L_{2m}(\xi) = (-1)^m BC_{2m}\cos\omega t\sqrt{\frac{2\pi}{\xi}}J_{2m+\frac{1}{2}}(\xi) \tag{6}$$

For m = 0 formula (6) gives the diffraction image of the ideal mirror, if one replaces cos by sin according to (2). It simply becomes:

$$L_0(\xi) = B\sin\omega t\frac{2\sin\xi}{\xi} \tag{7}$$

The shape of these diffraction images can be seen qualitatively from Fig. (4), which is valid for the analogous case of a circular mirror.

[6] See G. N. Watson, Bessel Functions, Cambridge 1922, pp. 50.

4. *Methods to make mirror surface errors visible.* To evaluate the image of the mirror surface we need the optical path length from the points of the intermediate surface to the points of the image surface. One finds the value $Constant + x_1 x'/s$ from (1) for the path length of a point x_1 on the intermediate surface to a point x' of the image surface. In order to find the light excitation M in the image surface we replace the t by $t - x_1 x'/s$ in L_n, take instead of B another amplitude constant and integrate over x_1. Since the Bessel function is odd in (5), and even in (6) and (7), one obtains (8)

$$M_{2m-1}(x') = -(-1)^m A' C_{2m-1} \cos\omega t \int_{-\infty}^{\infty} J_{2m-\frac{1}{2}}(\xi) \sqrt{\frac{2\pi}{\xi}} \sin x'\xi \, d\xi \tag{8}$$

$$M_{2m}(x') = (-1)^m A' C_{2m} \cos\omega t \int_{-\infty}^{\infty} J_{2m+\frac{1}{2}}(\xi) \sqrt{\frac{2\pi}{\xi}} \cos x'\xi \, d\xi \tag{9}$$

$$M_0(x') = A' \sin\omega t \int_{-\infty}^{\infty} \frac{2\sin\xi}{\xi} \cos x'\xi \, d\xi \tag{10}$$

The integrals appearing here yield hypergeometric functions of x'^2 according to the subsequently cited formula of Schafheitlin (16). One can find them more simply from the Fourier integral theorem: the L's are the Fourier transforms of the original oscillation $AC_nP_n(x)\cos\omega t$, and in the M's one finds the initial function back (multiplied by 2π), that is

$$M_n(x') = 2\pi A' \cos\omega t \, C_n P_n(x') \tag{11}$$

$$M_0(x') = 2\pi A' \sin\omega t \tag{12}$$

$$\text{for} - 1 < x' < +1$$

while the M's vanish outside of these boundaries. The result is that the oscillations (11) combine again to give an oscillation that is proportional to the mirror deviation d. By interference with (12) this oscillation yields the corresponding original phase deviations. So the image of the mirror surface agrees exactly in structure and phase with the light excitation of the mirror surface. Therefore one cannot observe deviations caused by the mirror errors without further aids.

One can make these phase deviations on the mirror surface visible in various ways by doing something to the intermediate image. In *one* method, one covers most of the diffraction image of the ideal mirror and lets through unhindered only the light diffracted by the errors (*dark field observation*). Our calculations show that this is potentially a very good method, since the diffraction disk of the ideal mirror and the diffraction images of the errors hardly overlap (see Fig. 4). In a *second* method, one covers half of the diffraction images caused by errors (*knife-edge or Schlieren method*). This method, due to Foucault [7] and Toepler [8], has so far usually been explained only

[7] Foucault, loc. cit.

[8] A. Toepler, Pogg. Ann. **131**, 33 (1867).

in terms of geometrical optics and therefore only for large surface errors [9]. The following diffraction theoretical calculation shows that there is a complicated relationship between the changes in intensity in the image and the changes in phase in the mirror surface.

A *third*, *new* method offers the advantage that small changes in phase in the mirror surface become visible as proportional changes in intensity in the image surface. This is obtained when one imparts a path difference of $\lambda/4$ to the diffraction image of the ideal mirror with respect to the other diffraction images in the intermediate surface (*phase-contrast method*). This means that $\sin\omega t$ is replaced by $\cos\omega t$ in formula (7) for the diffraction image of the ideal mirror, and that because of this the interference of (11) and (12) results in changes in amplitude rather than in phase.

5. *The knife-edge method.* Here we confine ourselves to the one-dimensional case as well. The calculation can be carried out most easily, if one simply covers half of the intermediate surface. The only change that appears in the calculation is that the integration over the intermediate surface now extends from 0 to ∞. Because of this the odd integrands also produce contributions, and instead of (8), (9), (10) one finds

$$N_{2m-1}(x') = \frac{1}{2}M_{2m-1}(x') + (-1)^m A' C_{2m-1} \sin\omega t \int_0^\infty J_{2m-\frac{1}{2}}(\xi)\sqrt{\frac{2\pi}{\xi}}\cos x'\xi\, d\xi \tag{13}$$

$$N_{2m}(x') = \frac{1}{2}M_{2m}(x') - (-1)^m A' C_{2m} \sin\omega t \int_0^\infty J_{2m+\frac{1}{2}}(\xi)\sqrt{\frac{2\pi}{\xi}}\sin x'\xi\, d\xi \tag{14}$$

$$N_0(x') = \frac{1}{2}M_0(x') - A'\cos\omega t \int_0^\infty \frac{2\sin\xi}{\xi}\sin x'\xi\, d\xi \tag{15}$$

According to Schaftheitlin [10], the integrals appearing here are discontinuous at $x' = 1$ and can be represented by hypergeometric functions according to the general formula

$$\int_0^\infty J_\mu(\xi)J_\nu(x\xi)\, d\xi \tag{16}$$

$$= \frac{\Gamma(\frac{1}{2}(\mu+\nu+1))}{\Gamma(\frac{1}{2}(\mu-\nu+1))\Gamma(\nu+1)} x^\nu F(\tfrac{1}{2}(\mu+\nu+1), -\tfrac{1}{2}(\mu-\nu-1), \nu+1, x^2)\ldots(|x|<1)$$

$$= \frac{\Gamma(\frac{1}{2}(\mu+\nu+1))}{\Gamma(\frac{1}{2}(-\mu+\nu+1))\Gamma(\mu+1)} x^{-\mu-1} F(\tfrac{1}{2}(\mu+\nu+1), \tfrac{1}{2}(\mu-\nu+1), \mu+1, x^{-2})\ldots(|x|>1)$$

In our case then for example

$$\int_0^\infty J_{2m+\frac{1}{2}}(\xi)\sqrt{\frac{2\pi}{\xi}}\sin x'\xi\, d\xi = \pi\sqrt{x'}\int_0^\infty J_{2m+\frac{1}{2}}(\xi)J_{\frac{1}{2}}(x'\xi)\, d\xi$$

[9] Lord Rayleigh, Phil. Mag. (6) **33**, 161 (1917) and S. Banerji, Astroph. J. **48**, 50 (1918) give the diffraction theory only for the ideal mirror and for simple discontinuous deviations.

[10] See Watson, Bessel Functions, pp. 284.

$$= \frac{\pi\Gamma(m+1)}{\Gamma(m+\frac{1}{2})\Gamma(\frac{3}{2})} x' F(m+1, -m+\tfrac{1}{2}, \tfrac{3}{2}, x'^2) \quad = \quad (-1)^m 2Q_{2m}(x') \ldots |x'| < 1$$

[11]

$$= \frac{\pi\Gamma(m+1)}{\Gamma(-m+\frac{1}{2})\Gamma(2m+\frac{3}{2})} x'^{-2m-1} F(m+1, m+\tfrac{1}{2}, 2m+\tfrac{3}{2}, 1/x'^2) \quad = \quad (-1)^m 2Q_{2m}(x')$$

$$\ldots |x'| > 1$$

[12] and analogously for the integral in (13). Q is the Legendre function of the second kind, which by conventional definition is given on the real axis by

$$Q_n(x) \quad = \quad \tfrac{1}{2} P_n(x) \log\left|\frac{1+x}{1-x}\right| - \frac{2n-1}{1\cdot n} P_{n-1}(x) - \frac{2n-5}{3(n-1)} P_{n-3}(x) - \ldots$$

We then have

$$\begin{aligned} N_{2m-1}(x') &= \pi A' \cos\omega t\, C_{2m-1} P_{2m-1}(x') + 2A' \sin\omega t\, C_{2m-1} Q_{2m-1}(x') \\ N_{2m}(x') &= \pi A' \cos\omega t\, C_{2m} P_{2m}(x') - 2A' \sin\omega t\, C_{2m} Q_{2m}(x') \\ N_0(x') &= \pi A' \sin\omega t - 2A' \cos\omega t\, Q_0(x') \end{aligned} \tag{17}$$

Covering half the diffraction image does not lead to an image of a mirror error $C_n P_n$ that agrees in structure and phase with the light excitation in the mirror surface, but rather to an oscillation that is superposed on the object-like image $\frac{1}{2} M_n$. This oscillation exhibits a phase difference of $\pi/2$, and its amplitude in the image surface has the shape of a Legendre function of the second kind Q_n.

In order to find the dependence of the intensity I in the mirror image, we must combine and square the terms with $\sin\omega t$ and likewise the terms with $\cos\omega t$ in (17). After omitting the unessential factor $\pi^2 A'^2$ we get within the geometrical image ($|x'| < 1$)

$$I_i \quad = \quad 1 - \frac{4}{\pi} \sum_3^\infty (-1)^n C_n Q_n + \frac{4}{\pi^2} Q_0^2 - \frac{4}{\pi} \sum_3^\infty C_n P_n Q_0 \tag{18}$$

where the quadratic terms in the coefficients C_n are omitted in agreement with earlier omissions. All object-like terms disappear outside the geometrical image ($|x'| > 1$) and only the ones with Q remain. With the same omission we have therefore

$$I_a \quad = \quad \frac{1}{\pi^2} \left(\log \frac{x+1}{x-1} \right)^2 \tag{19}$$

For the ideal mirror the intensity dependence is depicted in Fig. 2 according to (18) and (19). The absolute value 1 in the center of the mirror has the following meaning. The amplitude is equal to 2 and constant without the knife edge. The area of the intensity curve (rectangle) is equal to 8. The knife then takes away half the energy, so the area of the curve in Fig. 2 must be 4. Here 2 comes from the plotted rectangle and the other 2 from the bright borders. The calculation shows again that exactly a third of this falls inside the mirror surface [13]. The brightening of the borders is therefore not very disturbing.

[11] Heine, Kugelfunktionen 2nd ed. 1878, I, pp. 147.

[12] Whittaker & Watson, Modern Analysis, 4th ed. pp. 317.

[13] One finds by complex integration, that $\int_{-\infty}^{\infty} Q_0^2(x)dx = \frac{1}{2}\pi^2 \int_{-1}^{+1} Q_0^2(x)dx = \frac{1}{6}\pi^2$

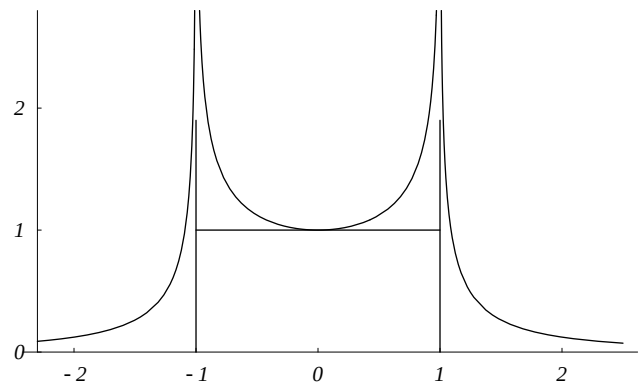

Figure 2: Intensity dependence of an error-free mirror under knife-edge test.

So what does a mirror error $C_n P_n(x)$ look like in this test? For even n, the deviations that appear, on the intensity distribution of the ideal mirror are, from (18) †

$$-\frac{4}{\pi}C_n\left(Q_n + \tfrac{1}{2}P_n \log\frac{1+x}{1-x}\right) \quad = \quad -\frac{4}{\pi}C_n\frac{1}{2^n n!}\frac{d^n}{dx^n}\left[(1-x^2)^n \log\frac{1+x}{1-x}\right] \tag{20}$$

for odd n, they are

$$\frac{4}{\pi}C_n\left(Q_n - \tfrac{1}{2}P_n \log\frac{1+x}{1-x}\right) \quad = \quad -\frac{4}{\pi}C_n\left[\frac{2n-1}{1\cdot n}P_{n-1}(x) + \frac{2n-5}{3(n-1)}P_{n-3}(x) + \dots\right] \tag{21}$$

This shows that in the first case the even function $P_n(x)$ is imaged as an odd function, and vice versa in the second case. Now one finds by the conventional geometrical optical treatment of the knife-edge test — which is obviously the correct one for the limiting case of large deviations — that the changes in intensity that become visible in the image are due not to height errors, but rather to slope errors of the mirror surface. Thus one finds the well-known appearance of an obliquely illuminated relief, which is adequate for qualitative purposes. In order to find the deviations of the mirror surface quantitatively, one would have to integrate the observed intensity curve. In order to judge the results of our calculation for small deviations, we have to integrate (20) and (21). As an example, the result for $n = 4$ is shown in Fig. 3, together with P_4. It can be shown in general that the integral has n roots, as does P_n, and is not too different from P_n/n ‡.

Every error $C_n P_n$ is therefore reproduced reasonably well. The factor $1/n$ causes higher ones to appear too weak in a series of errors. Consequently, sharp edges and jumps in the shape of $d(x)$ are reproduced as badly rounded.

6. Circular mirror. To be able to extend the preceding considerations to the practically important case of a circular boundary, we must first look for the corresponding orthogonal polynomials. These will then be used specifically to investigate the phase contrast method.

†Translator's note: a "−" sign, missing in the original article, has been added to the left side of Eqn. 20.

‡Translator's note: indeed, to arrive at the solid curve in Fig. 3, one must multiply the expression $-\frac{1}{2^4 4!}\frac{d^3}{dx^3}\left[(1-x^2)^4 \log\frac{1+x}{1-x}\right]$ by 4.

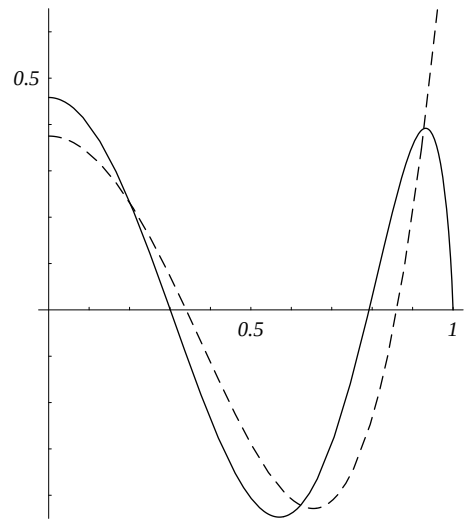

Figure 3: Mirror error P_4 (dashed curve) and its appearance in the knife-edge test (solid curve).

In order to arrive at polynomials that are orthogonal over a circular area ("circle polynomials"), we apply a rotationally invariant partial differential equation [14]. In its most general form such an equation can be written as

$$\Delta V + \alpha\left(x\frac{\partial}{\partial x} + y\frac{\partial}{\partial y}\right)^2 V + \beta\left(x\frac{\partial}{\partial x} + y\frac{\partial}{\partial y}\right)V + \gamma V \quad = \quad 0$$

The coefficient of the highest-order derivative can be made to vanish on the unit circle by a suitable choice of α ($\alpha = -1$), and the expression can be made self-adjoint by a suitable choice of β ($\beta = -2$). γ is the eigenvalue parameter. The equation can be readily separated in polar coordinates. We get $V = R(r)\begin{smallmatrix}\sin\\ \cos\end{smallmatrix} m\varphi$ with the differential equation for R

$$r(1-r^2)R'' + (1-3r^2)R' + \{\gamma r - m^2/r\}R \quad = \quad 0$$

This can be readily reduced to a hypergeometric differential equation, which gives a useful solution up to $r = 1$ in the form of a finite hypergeometric series (a Jacobi polynomial) only for $\gamma = n(n+2)$, $n - m$ even. We get

$$\begin{aligned} R_n^m(r) &= (-1)^{\frac{n-m}{2}}\binom{\frac{1}{2}(n+m)}{m} r^m F\left(\frac{n+m+2}{2}, -\frac{n-m}{2}, m+1, r^2\right) \\ &= \frac{r^{-m}}{\left(\frac{n-m}{2}\right)!}\left(\frac{d}{d(r^2)}\right)^{\frac{n-m}{2}}\left\{r^{n+m}(r^2-1)^{\frac{n-m}{2}}\right\} \end{aligned} \tag{22}$$

[14] In another way one finds these polynomials as a generalization of Legendre polynomials when one starts with the potential equation in 4 dimensions and determines the axially symmetrical solutions (zonal hyperspherical functions). This work will be carried out in more detail elsewhere. Translator's note: the mentioned work was later published as "Hypersphärische Funktionen und die in sphärischen Bereichen orthogonalen Polynome," F. Zernike and H. C. Brinkman, Proc. Kon. Akad. Wet. **38**, 161 (1935).

where the constant is so chosen that $R_n^m(1) = 1$. These polynomials as eigenfunctions are orthogonal over the unit circle, particularly

$$\int_0^1 R_n^m(r) R_{n'}^m(r) r\, dr \quad = \quad 0 \quad ,$$

$$\int_0^1 (R_n^m)^2 r\, dr \quad = \quad \frac{1}{2n+2}$$

The polynomials of the lowest orders may be explicitly stated as

$m\backslash n$	0	1	2	3	4	5	6
0	1		$2r^2-1$		$6r^4-6r^2+1$		$20r^6-30r^4+12r^2-1$
1		r		$3r^3-2r$		$10r^5-12r^3+3r$	
2			r^2		$4r^4-3r^2$		$15r^6-20r^4+6r^2$
3				r^3		$5r^5-4r^3$	
4					r^4		$6r^6-5r^4$
5						r^5	
6							r^6

The calculation of the diffraction image in the intermediate surface then proceeds exactly analogously to §3, with (3) replaced by the following series expansion for mirror deviations

$$\frac{4\pi}{\lambda} d(r,\varphi) \quad = \quad \sum_{n,m} (A_{nm} \sin m\varphi + B_{nm} \cos m\varphi) R_n^m(r)$$

The four terms B_{00}, A_{11}, B_{11}, B_{20} disappear by suitable adjustments. The subsequent ones correspond to real mirror deviations, such as $R_2^2 \sin 2\varphi = 2xy$ and $R_2^2 \cos 2\varphi = x^2 - y^2$ for astigmatism as well as R_4^0 for spherical aberration.

Analogous to (4), one finds the light excitation originating from the mirror error $B_{nm} R_n^m(r) \cos m\varphi$ in the point x_1, y_1 of the intermediate surface from the integral

$$L_{nm} \quad = \quad \int_0^1 AKB_{nm} R_n^m(r) \int_0^{2\pi} \cos m\varphi \cos \omega(t + (xx_1 + yy_1)/sc) r\, dr\, d\varphi$$

If one sets $\omega x_1/sc = \rho \cos\psi$, $\omega y_1/sc = \rho \sin\psi$ and $\varphi = \chi + \psi$, or $\omega(xx_1 + yy_1)/sc = r\rho \cos\chi$, one obtains for even n and m

$$L_{nm}(\rho,\psi) \quad = \quad AKB_{nm} \cos\omega t \cos m\psi \int_0^1 R_n^m(r) \int_0^{2\pi} \cos m\chi \cos(\rho r \cos\chi) r\, dr\, d\chi$$

since the integrals with $\sin m\chi$ or $\sin(r\rho\cos\chi)$ vanish. As generally known, the integral over χ yields a Bessel function of $r\rho$ and it remains to evaluate

$$\int_0^1 R_n^m(r) J_m(\rho r) r\, dr \quad = \quad (-1)^{\frac{n-m}{2}} \rho^{-1} J_{n+1}(\rho) \ . \tag{23}$$

One can find this by substituting the power series for $J_m(\rho r)$ and integrating term by term. This simple result can also be proven by the following calculation, since the diffraction image in the intermediate surface must reproduce the initial function in the image surface by the second diffraction. Mathematically expressed this means that if

$$\int_0^1 R_n^m(r) J_m(\rho r) r\, dr = f(\rho)$$

then conversely

$$\begin{aligned} \int_0^\infty f(\rho) J_m(r\rho)\rho\, d\rho &= R_n^m(r) \qquad r<1 \\ &= 0 \qquad r>1 \end{aligned} \tag{24}$$

by the Fourier-Hankel integral theorem [15]. According to the Schafheitlin formula (16), we then have

$$\begin{aligned} \int_0^\infty J_{n+1}(\rho) J_m(r\rho) d\rho &= \binom{\frac{m+n}{2}}{m} r^m F(\tfrac{1}{2}(n+m+2), \tfrac{1}{2}(m-n), m+1, r^2) \qquad r<1 \\ &= 0 \qquad r>1 \end{aligned} \tag{25}$$

with this formula (23) is proven by the use of (22) and (24). The diffraction image becomes then

$$L_{nm}(\rho,\psi) = (-1)^{n/2} 2\pi A K B_{nm} \cos\omega t \cos m\psi\, \rho^{-1} J_{n+1}(\rho)$$

and analogously for odd m and n and for terms with $\sin m\varphi$. The radial factor is independent of m. The diffraction image of the ideal mirror again has the other phase

$$L_{00} = 2\pi A K \sin\omega t\, \rho^{-1} J_1(\rho)$$

The radial amplitude dependence of the diffraction images is depicted in Fig. 4 for several values of n. To obtain the same dimension for the ordinate, a factor $2n+2$ was included. One sees that the higher order errors do not cause any noticeable change in the central part of the diffraction image of an error-free mirror ($n=0$). On the contrary, the higher the order is, the farther from the center its influence lies.

Without modification of the diffraction image, the mirror errors again cause only phase changes in the image surface, so that the mirror surface appears uniformly bright. The calculation of this second diffraction was already anticipated in formula (25) above. The formula for the error-free mirror is

$$\begin{aligned} M_{00}(r') = \frac{4\pi^2 K}{s\lambda} A \sin\omega t \int_0^\infty J_0(r'\rho) J_1(\rho) d\rho &= A\sin\omega t \qquad r'<1 \\ &= 0 \qquad r'>1 \end{aligned} \tag{26}$$

[15] Watson, Bessel Functions, pp. 453.

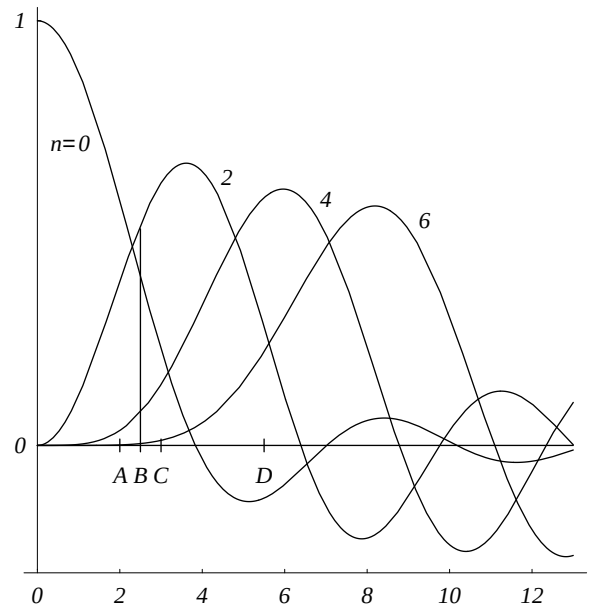

Figure 4: Diffraction images $(2n+2)J_{n+1}(\rho)/\rho$ for the circular mirror.

7. Phase contrast with circular mirror. To make the mirror errors visible, the diffraction image must be changed somehow. We consider here especially more closely the phase-contrast method, by which the phase of the central part of the diffraction image is changed by 90° from the remaining part. In this method, one puts a glass plate with a small, lowered or raised circular disk (phase-contrast disk) in the path of the rays and adjusts it to be exactly in the diffraction image. As one can see in Fig. 4, such a disk, whose edge may be located somewhere between A and D, practically does not change the higher order diffraction images. However, the question remains: to what extent can the zero order image be seen as having undergone a 90° phase change, as its diffraction rings do not experience this change. So for a small disk with radius a, two parts of the diffraction image have to be considered separately, i.e. the integral in (26) has to be evaluated from 0 to a and from a to ∞.

To evaluate the integral

$$I(r',a) \quad = \quad \int_0^a J_0(r'\rho)J_1(\rho)\,d\rho$$

one may represent $J_1(\rho)/\rho$ in the interval $0 \to a$ by a series of R-polynomials with the argument $\rho' = \rho/a$

$$J_1(\rho)/\rho \quad = \quad \sum k_{2n} R^0_{2n}(\rho') \quad ,$$

$$k_{2n} \quad = \quad (4n+2)\int_0^1 R^0_{2n}(\rho')\frac{J_1(a\rho')}{a\rho'}\rho'\,d\rho' \quad .$$

One inserts here the integral according to (25), and easily finds

$$k_{2n} = (-1)^n(4n+2)a^{-2}\int_0^a J_{2n+1}(x)\,dx$$

and further

$$I(r') = (1-J_0(a))2\frac{J_1(ar')}{ar'} + (1-J_0(a)-2J_2(a))6\frac{J_3(ar')}{ar'}$$
$$+(1-J_0(a)-2J_2(a)-2J_4(a))10\frac{J_5(ar')}{ar'} + \ldots$$

From this formula we calculated for $a = 2$, 2.5, and 5.5 the dependence of I over the mirror surface ($r' < 1$) and somewhat outside that, up to $r' = 1.2$, for which the 4 highest terms were sufficient. I is fairly constant, if $J_0(a) = 0$.

The light excitation which immediately after the reflection by the mirror is given by

$$A\sin\omega t + A\frac{4\pi}{\lambda}d(r,\varphi)\cos\omega t$$

(Formula 2) and by the same formula in the image plane with r' and φ' without phase contrast, is altered by the disk to

$$A(1-I(r'))\sin\omega t + A\left(I(r') + \frac{4\pi}{\lambda}d(r',\varphi')\right)\cos\omega t$$

and the image intensity becomes

$$A^2(I^2 + (1-I)^2) + 2A^2I\frac{4\pi}{\lambda}d \quad .$$

Therefore, the impossibility of changing the zero-order diffraction image everywhere by 90° has two draw-backs: *first* the deviations d of the mirror surface show up less strongly, because of the factor I, which, however, still amounts to 0.5 to 0.6 even for the smallest disk; *second* an error-free mirror is not seen as uniformly illuminated either. The intensity dependence $I^2 + (1-I)^2$ is illustrated in Fig. 5 for the above-mentioned three values of a corresponding to points A, B, and D in Fig. 4 [¶]. Accordingly smaller disks are to be preferred. But the exact size is not important, since one would e.g. in case B produce a practically uniform intensity by just a small change in focus.

For the practical use of mirror tests and the fabrication of phase-contrast disks one should consult the work by Burch [16].

Groningen, 30 April 1934.

[¶] Translator's note: to produce the curves in Fig. 5, one must use the correct intensity $2I^2$, not $I^2 + (1-I)^2$, for $r' > 1$.

[16] Burch, loc. cit.

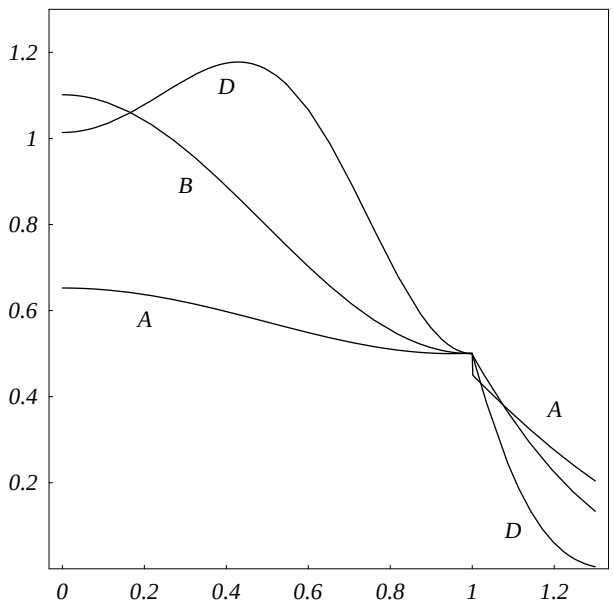

Figure 5: Intensity dependence of an error-free mirror under phase-contrast test.